Composite of TiO$_2$-montmorillonite from Indonesia and Its photocatalytic Properties in Methylene Blue and *E.coli* Reduction

Is Fatimah

Chemistry Department, Islamic University of Indonesia
Kampus Terpadu UII, Jl. Kaliurang Km 14, Yogyakarta, Tel: +6227489649 ext3011,

Abstract

Titania pillared montmorillonite from Indonesian montmorillonite by using titanium isopropoxide as precursor was successfully prepared. Physico-chemical character of material by using x-ray diffraction, gas sorption analyzer, diffuse reflectance UV-Visible, scanning electron microscope (SEM) and energy dispersive x-ray (EDAX) showed the dipersion of titania in dominantly anatase phase that is theoretically active as photocatalyst. The photoactivity was evaluated in methylene blue photodegradation and *Eschericia coli* inactivation. The kinetics of metylene blue photodegradation indicate the significant role of prepared material as photocatalyst as well as in *E.coli* inactivation. Photodegradation of methylene blue over prepared material shows the fitness to Langmuir-Hinshelwood model.

Keywords: Langmuir-Hinshelwood model, montmorillonite, pillared clay, photodegradation, titania

1. Introduction

Photocatalytic degradation of pollutant molecules from water and environment is an interesting technology refer to its low energy, minimum cost and less chemicals used within the technology. Among some photocatalyst, TiO$_2$ is the most popular material due to its high band gap energy (3.2eV) and less toxicity. Degradation of hazardous substances by TiO$_2$ is refer to reduction-oxidation reactions generated from absorption of photons by TiO$_2$ that leads photoexication: the formation of electron–positive hole pairs. A continous process under available photon source such as UV light from sunlight make it markedly effective for destroying toxic organic molecules in wastewater treatment [1,2]. However, some limitations present in the use of pure TiO$_2$ related to its minimum adsorptivity related to its low surface area affecting to reduce the photocatalyst efficiency. The use of stable and high surface area adsorbent in a composite form with TiO$_2$ is a strategy to overcome these problems. In advance, exploiting nanoparticle of photocatalyst on surface also affect to decrease the probability of recombination of electrons and positive holes in basic photoexcitation mechanism. Such immobilization also circumvents a problem that has emerged in using TiO$_2$ nanoparticles in suspension; the troublesome separation of nanoparticles after treatment. The use of silica-alumina materials as the support for TiO$_2$ was reported to be more effective by attracting higher concentration of target substances around the photo-catalyst sites from the support's adsorbability[3-5].

Minerals within the smectite class of clay are interesting support for TiO$_2$ refer to sweallability and easily to form composite by pillarization process. The formation of TiO$_2$ immobilized smectite clay within term pillarization involved the cation exchange between native cations in clay structure with polyoxication of metal as metal oxide precursor followed by calcination to form stable metal oxide. This scheme has been reported by previous investigations. Study on effect of some parameters in TiO$_2$-pillared clay synthesis and its application as photocatalyst in several reactions were   also conducted [6-8]. Considering that

montmorillonite clay is one abundant mineral in Indonesia, this research is aimed to investigate the use of Indonesian montmorillonite as support for TiO_2. In present work we have prepared the composite by using by using titanium isopropoxide as precursor of TiO_2. The chosen method was refer to some limitations of the use other titania precursors such as $TiCl_4$ and $TiOCl_2$ which are stable in a very low pH and have an excessive properties potentially destroy the structure of clay minerals [9]. Photocatalytic activity of prepared material was studied in the photodegradation efficiency of methylene blue and also in photo-inactivation of *Eschericia coli* (*E.coli*) bacteria.

2. Material and Method
2.1 Material
Natural occuring montmorillonite clay was obtained from PT. Tunas Inti Makmur Semarang, Indonesia. Acid activation by refluxing in a 0.1 N sulphuric acid solution for 6 hours followed by neutralization, drying and grinding was conducted before its used in composite formation. Titanium tetraisopropoxide (TTIP, 97%) was procured from Aldrich, USA. methylene blue (MB) was selected as model compounds in this study, which was purchased from E.Merck, Germany. Other chemicals such as H_2SO_4, isopropanol and ethanol in pro analyst quality were supplied from E.Merck.

2.2 Preparation and characterization of TiO_2 pillared montmorillonite
A TiO_2 precursor was synthesized by dispersing TTIP into isopropanol under vigorously sttirring to prevent the formation of agglomerates. The mixture was then added with HCl and stirring for 4 hous until a clear yellow solution was obtained. The solution was added droply into suspension of activated montmorillonite in water (5% wt.) followed by stirring for 24 hours. This mixture was then filtered, neutralized by using distilled water, dried by heating in oven at 100∘C for a night. Finally, the solid was calcined at 450∘C for 6 h. By this procedure, the solid obtained was assigned to as composite of TiO_2-montmorillonite (TiO_2/MMT).

The physico-chemical character of prepared material and raw montmorillonite was studied by x-ray diffraction, gas sorption analysis, Fourier-Transform infra red spectrophotometry (FTIR) and scanning electron microscope(SEM). X-ray powder diffraction patterns of TiO_2/MMT was obtained using Shimadzu X 6000 using $CuK\alpha$ radiation ($\lambda = 0.15405$ nm) in a 2θ range of 0–60. The pattern was compared with the standard anatase and raw montmorillonite.

2.3. Photodegradation of MB
Photodegradation experiments were conducted in a batch reactor consist of a 500 mL thermal stable glass reactor under UV light at the wavelength of 326nm. The distance between lamp and reactor is about 30cm. Photodegradations were engaged by dispersing a certain amount of photocatalyst powder into MB solution followed by stirring and UV illumination. The experiments were conducted at varied initial concentration of MB and determination of MB during treatment was performed by sampling at certain interval time sequentially and analyzed by using UV-Visible spectrophotometry and high performance liquid chromatography (HPLC) analysis. A Hitachi U2010 spectrophotometer and Shimadzu HPLC instruments were employed for these analysis. For Liquid Phase Chromatography (LPC) analysis, mobile phase of acetonitrile:water (1:1) at the flow rate of 1mL/minute, stationary phase of C8 and UV detector analytical conditions were set up. It should be noticed that the UV-light was turned on for photodegradation reaction and these experiments were calibrated by adsorption process which is the same treatment without UV light illumination. Previous statistical analysis confirm that by MB reduction adsorption can be negligible.

2.4. Antibacterial Test
E. coli inoculated in L-broth and cultured at $40^{o}C$ K for 18 h. The culture solution was collected by centrifugation (6500 rpm, 10 min, 277 K) and washed twice with demineralized water. Then, a test solution containing 7×10^7 CFU /mL was prepared using sterilized water. Each 0.1 of TiO_2/MMT suspension in triton-X and deionized water was layered on a 1cmx4cm glass. Then, the filmed glass was dried in oven at $100^{o}C$ for 24 h. Before was tested, the glass was cooled until it is in a normal room temperature. The glass was placed in culture solution in 100 ml Erlenmeyer flask under UV light illumination. Samples of treated solution were collected after 5 minutes, 30minutes and 60 minutes of illumination. Count of bacteria coloni was determined by agar method and counting was performed by automatic bacteria counter Scan 500.

3. Result and Discussion

3.1. Physico-chemical character of prepared material

Patterns of X-ray diffraction indicate the dispersion of titania does not affects much to structure of montmorillonite as shown by the presence of d001 reflection at around $2\theta = 6.24^o$, d_{020} and d_{006} at 19.78 and 35.42^o respectively (Figure 1). Compared to raw montmorillonite, these peaks were shifted from the reflections of montmorillonite which are placed at specific reflection of $2\theta = 6.3^o$ ($d_{001} = 14.9\text{Å}$) and other refections 19.89^o and 35.6^o corresponding to d_{020} and d_{006}. The shift of d001 reflection indicate the increased basal spacing of 0.14nm by the insertion of titania as propt of silicate sheets. The presence of titania are also appeared from the reflections corresponding to mixed chrystal of anatase (A) and rutile(R) phase.
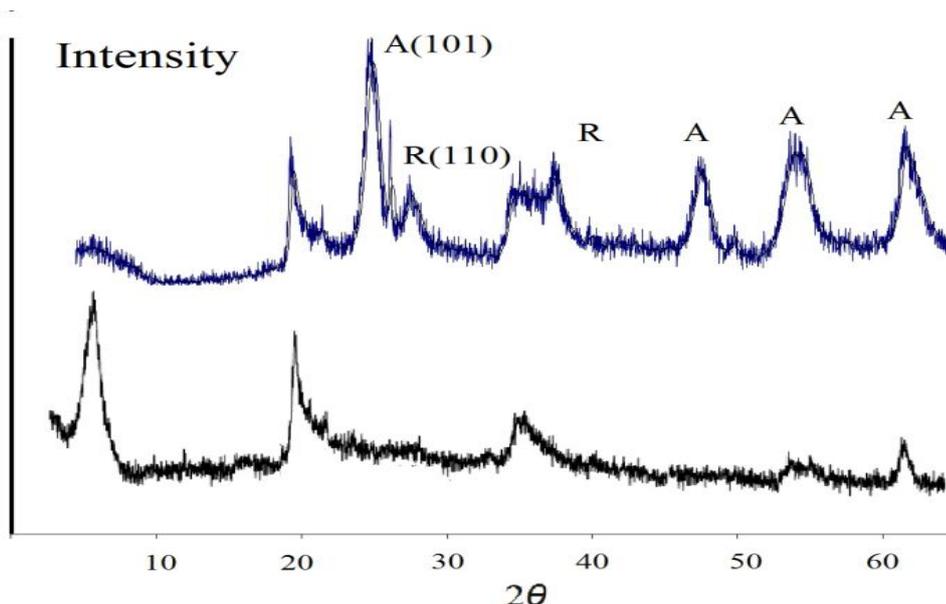
Figure 1: XRD pattern of raw montmorillonite (below) and TiO_2/MMT (above)

The identification of crystalline phase of TiO_2 as anatase at $2\theta = 25\cdot31$ (101) and rutile at $2\theta = 27\cdot41$ (110) was accomplished by comparison with a TiO_2 standard as reported by previous researches [10-11]. The presence of both phases in the dominancy of anatase phase exhibits the sol-gel mechanism of TiO_2 formation during pillarization process give tendency to form anatse structure from hydrolysis of titanium isopropoxide by the presence of acid in solution. Thermal treatment of intercalated montmorillonite during the calcination process accelerate the transformation of anatase to rutile [12]. The change of structural bonds in material is shown by FTIR spectra (Figure 2). Compared to raw montmorillonite TiO_2/MMT shows the higher wavenumber of around 1630cm^{-1} correspond to stretching vibration of the hydroxyl group and the interlayer water molecules indicate to the interaction of Si with Ti in structure as well as the spectrum at around 3430cm^{-1}. The important band at 920cm^{-1} that is found in TiO_2/MMT is attributed to the vibration of Si–O --- Ti from the polarized Si–O bond. Similar analysis and result was reported by similar preparation [13,14].

Compared to the raw montmorillonite, surface profile of TiO_2/MMT changed considerably after treatment of titania dispersion. Micrograph demonstrates the formation of titania particles creating porous structure on surface in line with nitrogen adsorption-desorption profile (Figure 3). The structural parameters calculated from the adsorption-desorption profile are listed in Table 1. The specific surface area of prepared TiO_2/MMT is extremely increased by TiO_2 dispersion (174.79m^2/g) refer to that of raw montmorillonite (45.11m^2/g). Result of elemental analysis from energy disperssive x-ray spectra (EDAX) (Figure 4) is listed in Table 2.
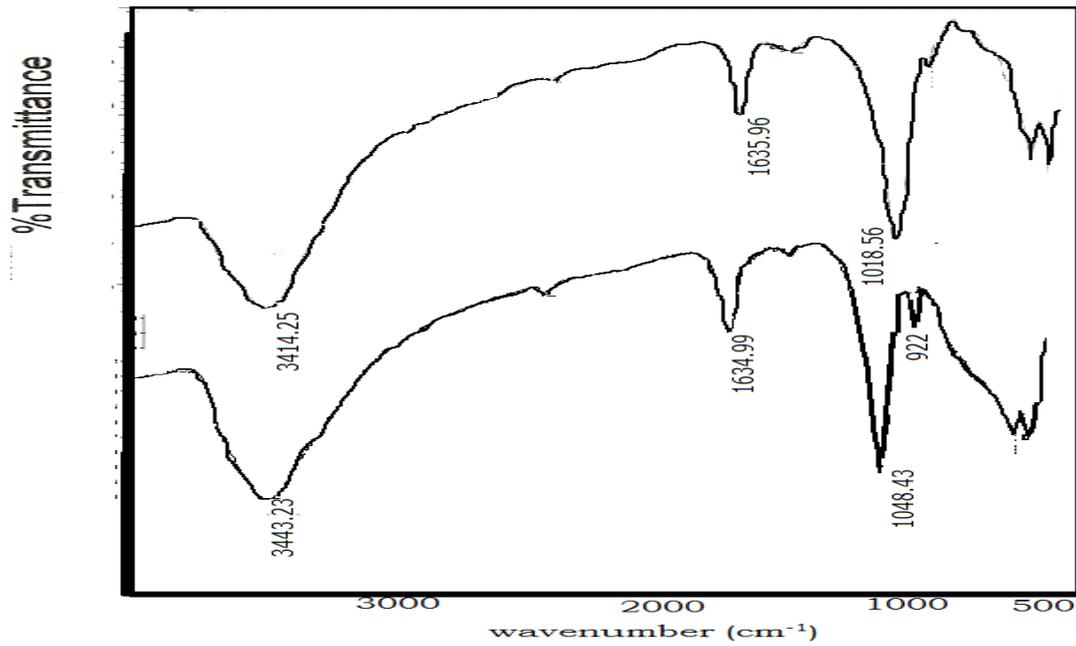
Figure 2: FTIR spectra of raw montmorillonite and TiO$_2$/MMT
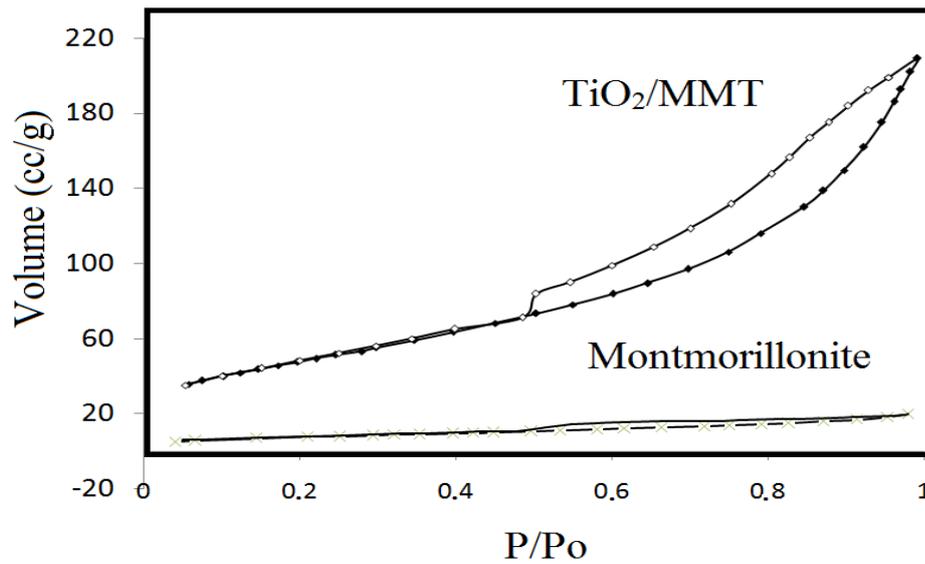
Figure 3: Adsorption desorption profile of raw montmorillonite and TiO$_2$/MMT

Table 1: Specific surface area, pore volume and pore radius of materials

Parameter	montmorillonite	TiO$_2$/MMT
Specific Surface area (m^2/g)	45.11	174.79
Pore volume (cc/g)	6.24×10^{-3}	3.24×10^{-1}
Pore radius ( )	15.90	37.07

It is noted that titania content in prepared material is 7.94 %wt., less than the amount dispersed (10%wt.). It is refer to that intercalation process is an equillibrium interaction so titanium ion is still in intercalating solution. Furthermore after the intercalation process washing and calcination process was conducted and produce less titanium dispersed in prepared TiO$_2$/MMT.

In spite of this, the pore volume of TiO$_2$/MMT is about 50 times greater compared to montmorillonite. The drastically changes upon titania pillarization is also been observed and reported by several previous investigations [7-8,13]. According to adsorption-desorption profile of isotherms indicating

the type IV in BDDT classification, it means that both micro and mesopores. The increased surface profile is addressed by mesoporous formation from TiO_2 particles on surface that is also in line with characteristic reflections appeared from XRD analysis. This result is different with what was reported by previous investigation for the same preparation with the same titania precursor; titanium tetraisopropoxide[8].

Table 2: Result of elemental analysis by using EDAX

Component (%wt.)	montmorillonite	TiO$_2$/MMT
Na$_2$O	8.33	1.13
MgO	3.39	5.44
Al$_2$O$_3$	21.62	17.56
SiO$_2$	59.80	54.25
FeO	3.58	0.12
CaO	0.58	0.18
Ti	-	7.94
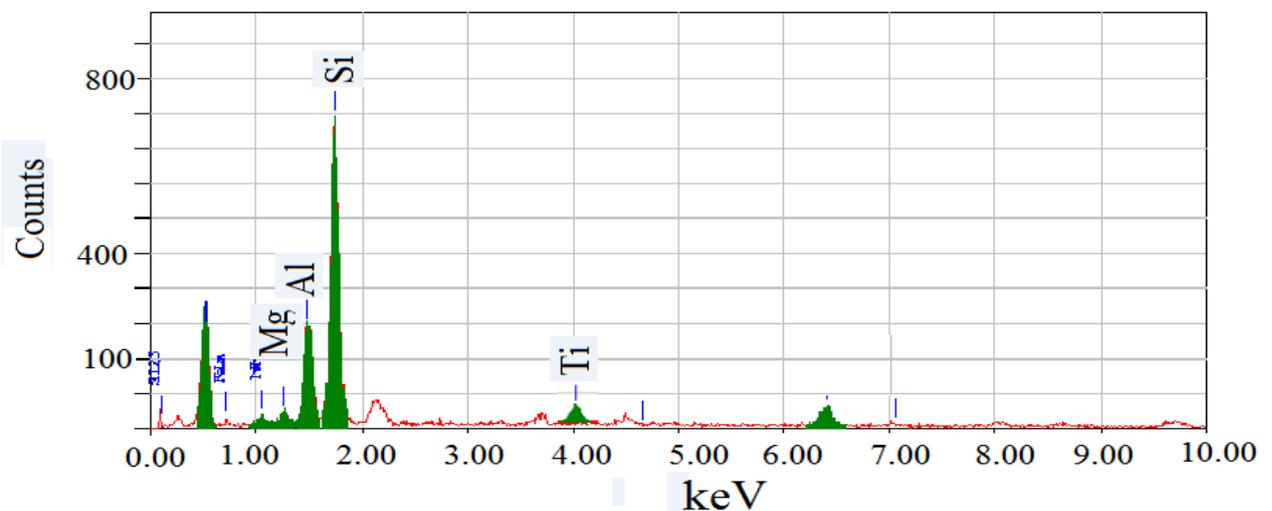
Figure 4: Spectral identification of TiO$_2$/MMT by EDAX analysis

Unless the concentration of Ti in TiO$_2$/MMT this research (Ti=7.94%)is slightly higher compared to Ti content in Ti-pillared bentonite prepared (TiO$_2$=12.36, Ti =7.40%), some differences with this result were appeared. In refered investigation, intense peaks correspond to TiO$_2$ formation in prepared material was not expressed by XRD analysis. Different content of clay mineral is the most responsible factor for different interaction between titania precursor and clay mineral. However the higher values of specific surface area and pore volume of prepared material compared to raw material indicates that titania particles are successfully attached to the structure of clay mineral. Since the surface area and volume of pores are critical reason for composite preparation, the data data indicate that the interlayer space of montmorillonite is more ccessible for the nitrogen molecule. The increased surface area is related to surface profile as presented by SEM micrograph suggesting the formation of porous titania on montmorillonite surface (Figure 5).

The evidence of created titania photocatalytic sites is showed by spectra of Diffuse reflectance-UV Visible absorption (Figure 6). An edge wavelength in the reflectance spectra of 375–250 nm is shown by TiO$_2$/MMT which edge wavelenght of 385.7nm lower value compared to the edge wavelength of TiO$_2$ P25 as a standard (389.4nm) while the raw montmorillonite give no intense absorbance within the range of measurement. This means the blue-shift effect as result of size quantitation effect by titania immobilization. Similar results were reported in titania pillared montmorillonite and titania pillared saponite and also immobilized TiO$_2$ in aluminium pillared montmorillonite [8,15,17]. This suggests the potency of prepared material to catch UV-Visible light and creating electron excitation which is the basic of photocatalysis mechanism.
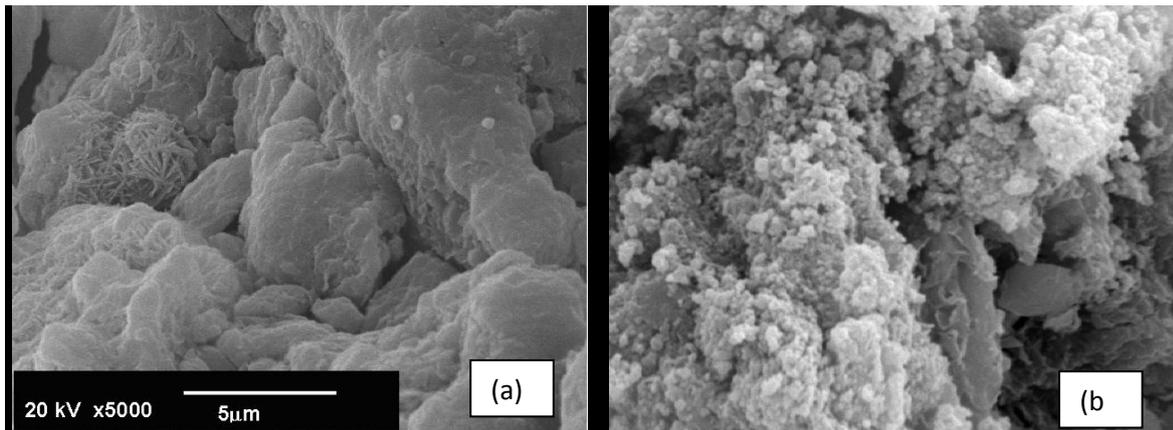
Figure 5: SEM profile of (a) montmorillonite and (b) TiO$_2$/MMT
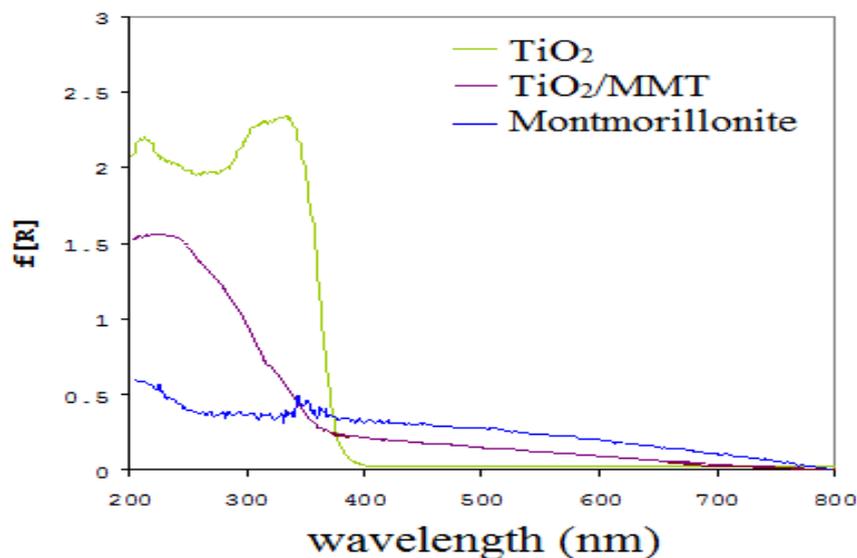
Figure 6: DRUV-Vis Spectra of montmorillonite, TiO$_2$/MMT and TiO$_2$ P25

3.2. Photocatalytic Activity in MB photodegradation
The kinetics of MB photodegradation at varied initial concentation are shown in Figure 7. The kinetic curve is constructed by plotting time of treatment Vs ratio of MB concentration at measured time respect to initial concentration of MB (C/Co). It can be seen that the kinetics of methylene blue photodegradation was very fast, with an equilibrium time of about 2 h. It was noted and interesting to gained that almost 50% (C/Co = 0.5) of the methylene blue was adsorbed within the first one minute of the contact time. From varied concentration, the data were simulated by Langmuir and Langmuir-Hinshelwood kinetics model. The selection of the models was based on the involvement of adsorption process within the whole mechanism and also refer to some kinetics studies by using clay based material. It is found that -Hinshelwood model is fitted well to the kinetics compared to Langmuir model (Figure 8 and Table 3). Equation of Langmuir Langmuir-Hinshelwood model are presented in eq.1 and eq.2.

$$q_e = \frac{q_m b C_e}{1 + b C_e} \qquad (1)$$

where Ce (mg/L) is the equilibrium concentration of MB and qe (mg/g) is the amount adsorbed/degraded MB dye per unit mass of the photocatalyst., qm (mg/g) in Langmuir equation is the maximum amount of MB per unit mass of photocatalyst corresponding to complete coverage of the adsorption sites, and b (L/mg) is the Langmuir constant related to the energy of adsorption.

$$\frac{1}{r_0} = \frac{1}{k} + \frac{1}{kK[MB]_0} \tag{2}$$

r_o = initial rate of MB photodegradation (L.min/mg), $[MB]_o$ = initial rate of MB, k= apparent rate constant (mg/L.min) and K = Langmuir-Hinshelwood constant.

Table 3: Calculated parameters of simulated Langmuir and Langmuir-Hinshelwood model

Isotherm Model	Parameter		Coefficient of determination (R^2)
	Parameter	Value	
Langmuir	qe	80.55	
	b	21.95	0.9276
Langmuir-Hinshelwood	1/n	0.1328	
	k	1.04×10^{-2}	
	K	11.49	0.9883
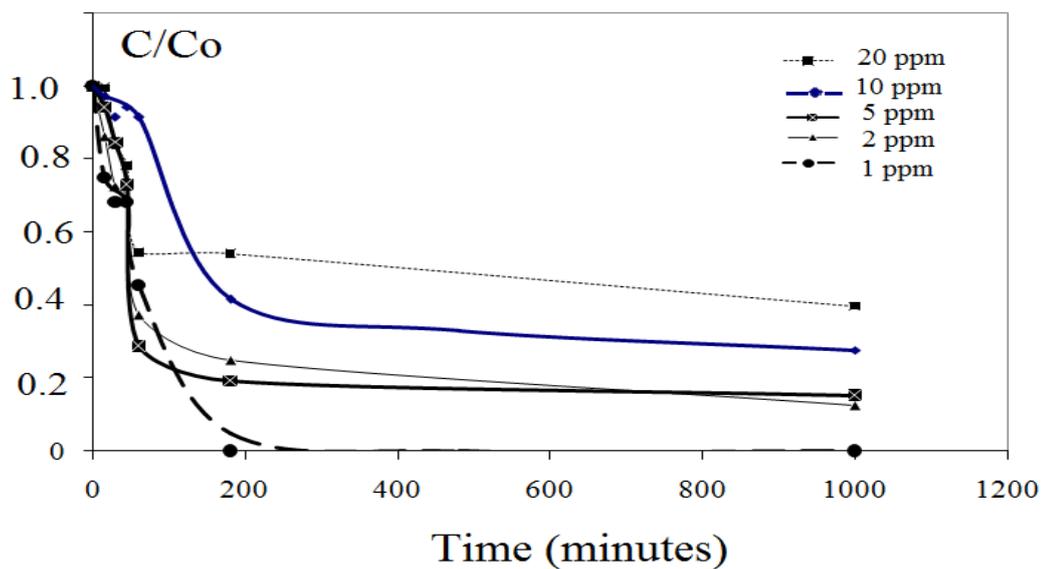
Figure 7 : Effect of initial concentration of MB to the photodegradation kinetics (photocatalyst dosage: 0.5g/L, UV light 326nm, C = concentration of MB at measured time, Co = initial concentration of MB)
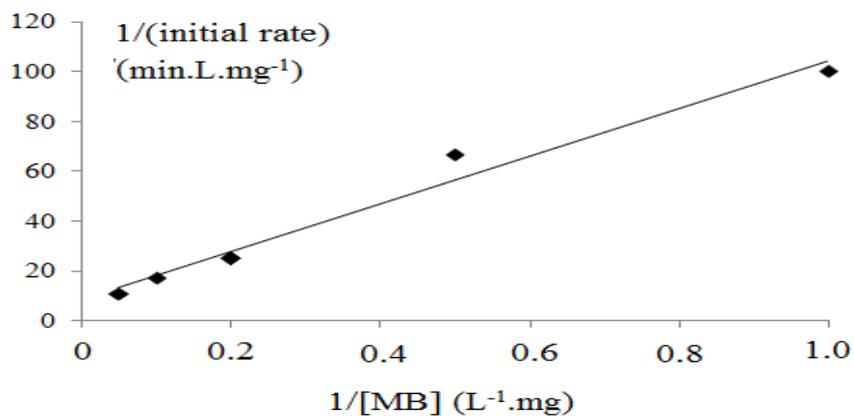
Figure 8: Langmuir-Hinshelwood plot of MB photodegradation kinetics by using TiO_2/MMT (catalyst dosage: 0.5g/L, initial concentration of MB=20mg/L)

In order to ensure that MB reduction by TiO$_2$/MMT is caused by photodegradation mechanism, spectrophotometric and chromatographic analysis to the treated solution was conducted. UV-Visible spectra of treated solutions by using montmorillonite and TiO$_2$/MMT (Figure 9) suggests the structural degradation towards methylene blue molecule. After was treated for 30 minutes, absorbance of characteristic spectra (270nm and 663.5nm) were decreased as indication of adsorption process without any structural changes to the molecule. In advance, as shown by spectra of treated solution after 60 minutes and 180 minutes it was shown that there is decreasing absorbance of spectrum at 663.5nm in coincise with the new spectra at around 290nm and 306nm which are responsible for the presence of aromatic structure. New peaks in treated solution are the evidences of the presence of new molecules as result of degradation. It is confirmed by LPC data (Figure 10). Untreated MB solution (initial) shows the sigle peak of MB molecule at retention time of 3.093 minutes and after was photocatalytic treated over TiO$_2$/MMT for 60 minutes, there are some new peaks of chromatogram   at 2.456 minutes, 6.260 minutes and 6.760 minutes from the occurence of the photodegradation products. Based on spiking and qualitative analysis to the treated solution, it is confirmed that the peak at 6.260 minutes is correspond to phenol. It is noticable that structure reduction of MB molecule potentially produce phenol as an intermediate for further smaller degradation products.
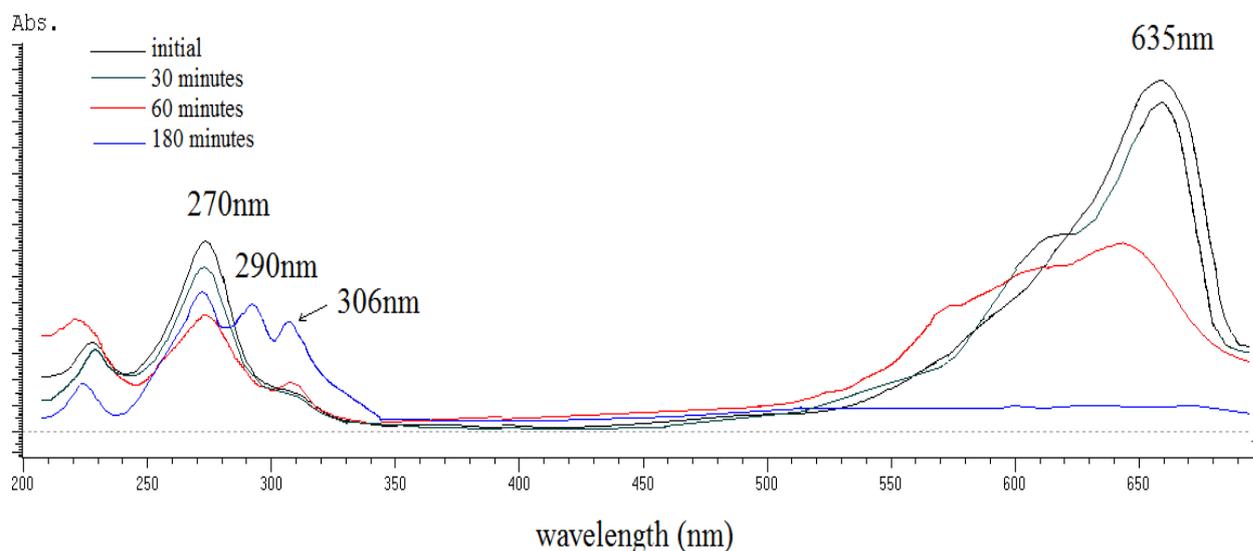
Figure 9: UV-visible spectra of treated   MB solution by using photodegradation over TiO$_2$/MMT(catalyst dosage: 0.5g/L, initial concentration of MB=20mg/L)
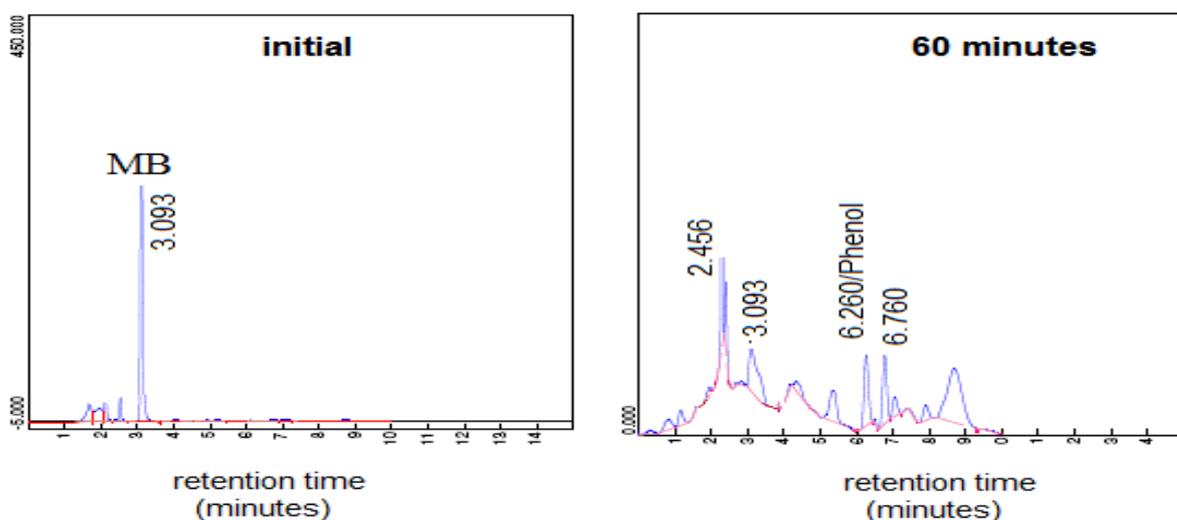
Figure 10: Result of LPC analysis toward treated MB solution by using photodegradation over TiO$_2$/MMT(catalyst dosage: 0.5g/L, initial concentration of MB=20mg/L)

Effect of Photocatalyst dosage

In the photocatalysis mechanism, photon is an important factor in generating radicals. Intensively the effect of photocatalyst dosage to the photodegradation rate was studied at the range of 0.5-2g/L. From the plot of initial rate vs. photocatalyst dosage (Figure 11) it is found that the optimum photocatalyst concentration is 0.5g/L. At lower dosage (2.5g/L) the rate is slower refer to the lower surface area and photoactive speciess available from photocatalyst amount that is kinetically affecting to accelerate the radical formation. However, the rate is also decreased at the addition of photocatalyst amount (1-2g/L). Refer to some previous investigations on photocatalysis by using photocatalyst powder, the lower rate corresponds to the limited UV light access caused by turbidity of solution at higher dosage.
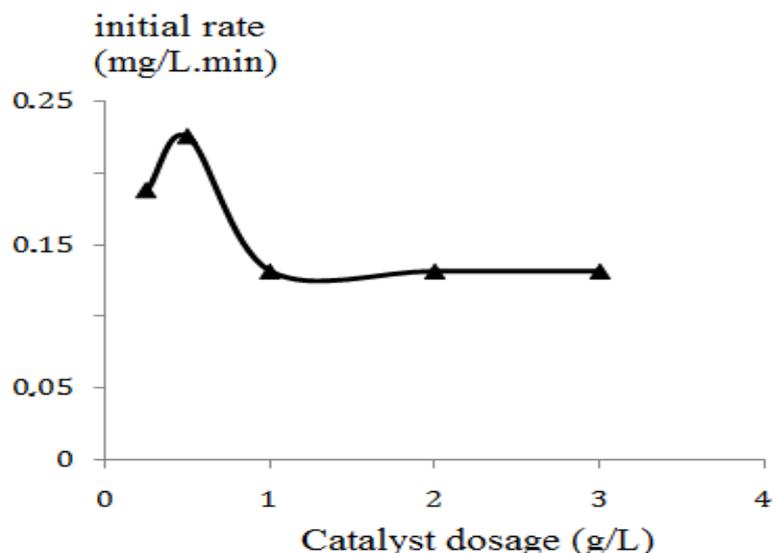
Figure 11. Effect of catalyst dosage to initial rate of MB photodegradation by TiO_2/MMT(initial concentration of MB=20mg/L)

3.3. Photoactivity in desinfection of E. coli

Photocatalytic antibacterial action of TiO_2/MMT was investigated by agar method of and killing kinetics methods using *E. coli* as a model bacteria. Compared to raw montmorillonite, TiO_2/MMT shows the appreciable inactivation as shown by decreasing colony count during the photocatalytic treatment over photocatalyst film (Figure 12).
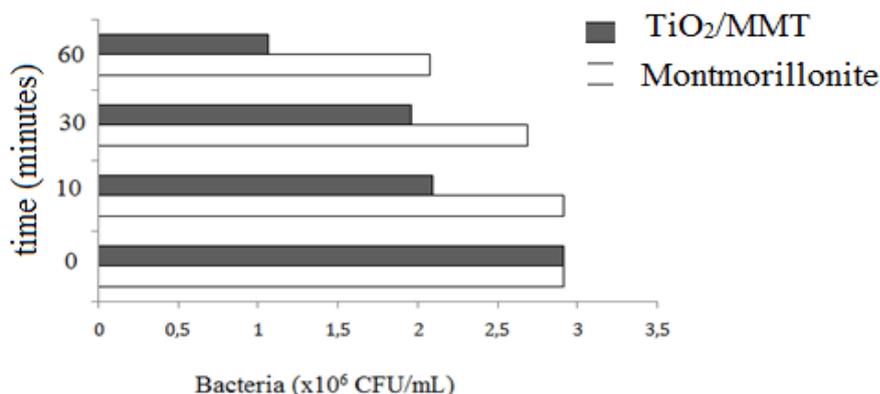
Figure 12: Bacteria growth after treatment using photocatalyst film of montmorillonite and TiO_2/MMT

According to similar research on photocatalytic desinfection by semiconductor metal oxide such as mechanism of antibacterial action by TiO_2 and ZnO nanoparticles, the desinfection was performed by the presence of reactive oxygen species such as hydroxyl radicals and superoxides that was produced by the contact between light and active sites of photocatalyst. Since the the hydroxyl radicals and super oxides are produced, its direct contact with the outer surface of bacteria could damage to proteins, lipids, and DNA [18-22].

Conclusion
Photocatalyst of TiO_2–pillared montmorillonite from Indonesia was successfully prepared. Prepared material exhibits the important physico-chemical character such as higher specific surface area and band gap energy as responsible parameter in its performance as photocatalyst. Photodegradation of methylene blue demonstrate that the photocatalytic reaction obey Langmuir-Hinshelwood model suggesting that the reaction is depend on adsorption mechanism. Prepared material has significant photoactivity in *E. coli* desinfection as shown by desinfection rate of bacteria culture solution over photocatalyst film of prepared material.

References

1. Fujishima, A., Zhang,X., Tryk, D.A., *International Journal of Hydrogen Energy*, 32 (2007) 2664.
2. Bhatkhande,D.S., Pangarkar, V.G., Beenackers, A., *Int.J.Chem.Tech.Biotechnol*. 77 (2001) 102.
3. Reddy,E.P., Davydov, L., Smirniotis, P., *Appl. Catal.B.,* 42 (2003) 1
4. Xu, Z., Xie, Q., Shou, C., Hui-min, Z., Yu, L., J. Environ. Sci. 19 (2007) 358.
5. Miao,S., Liu,Z., Han,B., Zhang, J., Yu,X., Du, J., Sun, Z, *J. Mater. Chem.* 16 (2006) 579.
6. Damardji, B., Khalaf, H., Duclaux, L., David, B, Appl. Clay Sci., 44 (2009) 201.
7. Okoye, I.P., Obi, C., *Res. J. Appl. Sci.* 6 (2011) 443.
8. Ding, Z., Kloprogge, J.T., Frost, R.L., Lu, G.Q., Xhu,H.Y., J. Por. Mater. 8 (2001) 273.
9. Yuan, P. He, H., Bergaya, F. Wu, D. Zhou, Q., Zhu, J. *Micro. Meso. Mater.*88 (2006)8.
10. Anpo, M., Nakaya, H., Kodama, Y., Domen, K., Onishi, T., *J.Phys.Chem*, 90(1986) 1633.
11. Mahadwad, O.K., Parikh, P.A., Jasra, R.V., Patil, C., *Bull. Mater. Sci*. 34(2011) 551.
12. Parra, R., Góes,M.S., Castro, M. S., Longo, E., Bueno, P. R., Varela, J. A., *Chem.Matter.,* 20(2008) 143.
13. Liu ,L., Li,X., Zuo,S., Yu, Y. *Appl. Clay Sci.* 37 (2007) 275.
14. Ninness, B.J., Bousfield, D.W., Tripp, C.P., *Colloids Surf., A Physicochem. Eng. Asp*. (2004)214, 195.
15. Kitayama, Y. , Kodama, T., Abe, M., Shimotsuma, *J. Por. Mater*., 5(1998) 121.
16. Yamanaka, S., Makita, K., *J. Por. Mater*. 1(, 1995) 29.
17. Lin, J., Jong, S., Cheng, S, *Microporous Materials,* 1 (1993) 281.
18. Fatimah, I., Wang, S. Narsito and Wiyaya,K., *Appl. Clay Sci.*, 50 (2010) 588.
19. Özdemir ,G., Limoncu ,M.H., Yapar, S., *Appl. Clay Sci.*, 48(2010) 319.
20. Vala´sˇkova´, M., Hunda´kova´ , M., Kutla´kova´,K.M., Seidlerova´,J., Cˇ apkova´, P., Pazdziora, E., Mateˇjova´, P., Herˇma´nek, K., Klemm, V., Rafaja, D., *Geochimica et Cosmochimica Acta* 74(2010) 6287.
21. Rengifo-Herrera , J.A., Mielczarski, E. , Mielczarski, J., Castillo, N.C., Kiwi, J., Pulgarin, C., *Appl. Cat. B.* , 84 (2008) 448.
22. Tankhiwale,R., Bajpai, S.K., *Coll. Surf. B.* 90 (2008)16.

(2012) http://www.jmaterenvironsci.com/